



Optics Letters

Measuring vibrations using Doppler shifted frequency modulated continuous-wave LIDAR with single photons

THEODOR STAFFAS,*  JULIA WOLLTER,  ALI W. ELSHAARI,  AND VAL ZWILLER

KTH Royal Institute of Technology, Department of Applied Physics, AlbaNova University Center, Roslagstullbacken 21, Stockholm 106 91, Sweden

*tstaffas@kth.se

Received 9 October 2024; accepted 15 December 2024; posted 16 December 2024; published 10 January 2025

We demonstrate a *frequency modulated continuous-wave (FMCW) light detection and ranging (LIDAR) system utilizing a superconducting nanowire single-photon detector (SNSPD) to measure vibrational spectra using reflected signals at the single-photon level. By determining the time-variant Doppler shift of the reflected probe signal, this system successfully reconstructs various audio signals, including pure sinusoidal, multi-tonal, and musical signals, up to 200 Hz, limited by the laser frequency modulation rate and the Nyquist sampling theorem. Additionally, we employ scanning galvo mirrors to perform 3D measurements and map audio signals from different regions in the scanned field of view. The integration of an SNSPD provides significant advantages such as near-unity detection efficiency, low dark count rates, and picosecond timing jitter, enabling measurements of vibrational spectra with as few as 100 detected reflected photons per laser sweep.*

© 2025 Optica Publishing Group under the terms of the [Optica Open Access Publishing Agreement](#)

<https://doi.org/10.1364/OL.544481>

Introduction. *Light detection and ranging (LIDAR)* is a technology that measures distances optically. It was first pioneered in the 1960s by militaries worldwide to be used as range finders for artillery [1]. Since its inception, it has also found widespread use in civilian applications [2], greatly impacting fields ranging from forestry [3] and mining [4] to space exploration [5] and climate research [6–8]. Originally, LIDAR systems relied solely on time of flight measurements of laser pulses and were limited to only determining distances between objects [1,9]. Subsequent improvements in various LIDAR components and analytical capabilities enabled LIDAR systems to determine objects' distances and perform other measurements such as reflectance [10], polarization mapping [11], or relative velocity [12]. One such improvement came in the form of *frequency modulated continuous-wave (FMCW) LIDAR*, which relies on measuring the interference between the reflected probe signal and a local reference oscillator. If the laser frequency is linearly modulated, the interfered signal intensity exhibits a beating frequency proportional to the target distance [9]. Furthermore, if

the target is moving, the reflected probe signal will experience an additional Doppler shift proportional to the target's velocity relative to the observer, affecting the resulting beating frequency of the interfered signal. This additional information allows for simultaneous measurement of the target's velocity and distance [13], and by tracking the modulation of the Doppler shifted signal, it is possible to determine the vibrational frequency of an object [14]. Furthermore, as FMCW LIDAR depends on the interference between two coherent signals, it is inherently insensitive to incoherent noise such as ambient light or detector noise. Another great advancement for the LIDAR field has been the rapid development of *superconducting nanowire single-photon detectors (SNSPDs)*. Integrating SNSPDs into LIDAR systems offers several advantages compared with other single-photon detectors, such as near-unity detection efficiency, no afterpulsing, low dark count rates, and picosecond timing jitter [15,16]. These advantages have enabled LIDAR measurements, using SNSPDs, over long range [17], with high accuracy [18], as well as through strongly scattering media such as water [19] or a human tissue [20]. In this article, we propose and construct an FMCW LIDAR setup utilizing a single SNSPD to measure the distance to an object and its vibrational frequency, by measuring the time varying Doppler shifted signal. We demonstrate the principle by measuring and reconstructing various audio signals applied to a speaker, including single- and multi-frequency signals as well as musical signals. Additionally, we perform 3D scans, mapping vibrational frequencies emitted from various regions in the scanned field of view.

Theory and experimental setup. Figure 1 presents the experimental setup used in this project and illustrates the FMCW LIDAR principle for both stationary and moving targets. In Fig. 1(a), a frequency modulated continuous-wave laser with 1550 nm central wavelength and <3 kHz linewidth (TOPTICA CTL 1550 nm) emits a signal via an optical fiber and a *collimating lens*, CL1, into a free-space setup, where the laser is split in two by *beam splitter 1 (BS1)*. The first portion serves as a local reference signal, Tx, which is passed through an attenuator and directed toward BS2. The second portion serves as a probe signal and is directed toward a target, in this instance a speaker, which vibrates with some applied signal. The reflected probe signal, Rx, is then directed by BS3 toward BS2 where it interferes with Tx. To compensate for losses in the Rx path the

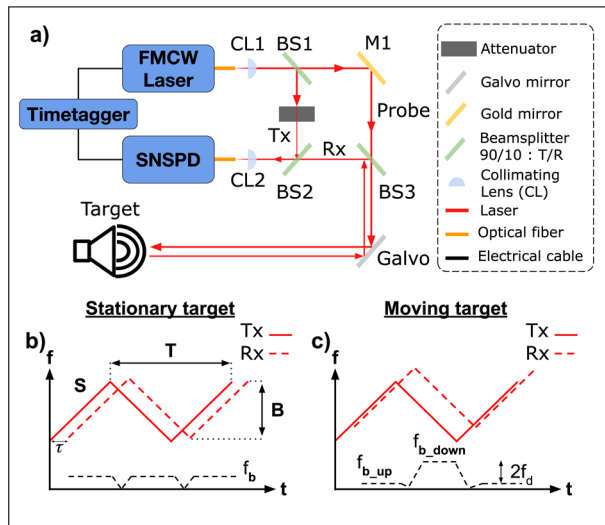


Fig. 1. (a) Sketch of our FMCW LIDAR setup. (b) Illustration of the FMCW principle for a stationary target. (c) Illustration of the FMCW principle for a target moving toward the observer. The Doppler effect shifts the reflected signal frequency and affects the beating frequencies of the up sweep and down sweep in opposing directions.

attenuator in the Tx path ensures that Tx and Rx signal intensities are balanced when interfering at BS2. The recombined signal is then coupled via an optical fiber to an SNSPD (Single Quantum, Eos detection system) with 20 ps timing jitter and 80% detection efficiency that measures the single-photon flux, which is recorded by a timetagger with 2 ps timing jitter (Swabian Timetagger X). The timetagger also receives electrical marker signals from the laser controller (TOPTICA, DLC pro), allowing for the recorded photon count rate to be separated according to the modulation direction of the laser, i.e., up sweep and down sweep. The galvo mirrors (Thorlabs GVS002) allow the probe signal to be scanned across a field of view in a point-to-point raster pattern by controlling the pitch and yaw of the optical path. The galvo controller unit (Labjack T7, with LJTick-DAC extension) also emits marker signals when changing positions that are recorded by the timetagger, allowing the recorded data to be split for each point under investigation.

The difference in path length for Rx and Tx between splitting at BS1 and recombining at BS2 causes a time delay, τ , between the two signals. When the laser's output frequency is linearly modulated, by applying an electrical triangular signal to a piezo crystal modulating the laser cavity, over a given bandwidth, B , as shown in Fig. 1(b), the time delay results in Tx and Rx having different frequencies at BS2. The recombined signal intensity will therefore exhibit a beating frequency, f_b , equal to the difference in laser frequency of the Rx and Tx signals, given by Eq. (1), where S is the frequency slope, as shown in Fig. 1(b), c is the speed of light, and d is the distance to the object:

$$f_b = |S\tau| = \left| \frac{S2d}{c} \right|. \quad (1)$$

Important to note is that Eq. (1) is only valid for stationary objects. For moving objects, the Rx signal frequency is Doppler shifted (given that there is a velocity component parallel to the probe signal's optical path). As illustrated in Fig. 1(c), the Doppler shift affects the beating frequency of the up and down

sweep with opposite signs, shifting them by a magnitude given by Eq. (2), where λ is the laser wavelength and v is the parallel relative velocity between the observer and the object (positive velocity is defined toward the observer). Strictly speaking, the value of λ changes during the frequency modulation, affecting the Doppler shift. However, this effect is orders of magnitude smaller than the effect of the velocity for any practical application, and therefore λ is considered constant in our analysis. The result of the Doppler shift is that the beating frequencies for the up sweep, $f_{b_{up}}$, and down sweep, $f_{b_{down}}$, are shifted according to Eqs. (3) and (4):

$$f_d = \frac{2v}{\lambda}, \quad (2)$$

$$f_{b_{up}} = \left| \frac{S2d}{c} - f_d \right|, \quad (3)$$

$$f_{b_{down}} = \left| \frac{S2d}{c} + f_d \right|. \quad (4)$$

These equations demonstrate that we can sample an object's velocity and distance with a single modulation laser sweep, i.e., we sample these values at a frequency, $f_s = \frac{1}{T}$, where T is the period of the laser modulation as shown in Fig. 1(b). The aim is now to measure the vibration of the speaker in Fig. 1(a), placed at ≈ 50 cm distance. The momentary velocity, $v(t)$, is the time derivative of the vibrational signal, $x(t)$, and assuming this can be written as a superposition of sinusoidal signals, $x(t)$ and $v(t)$ are given by Eqs. (5) and (6), where A_i and ω_i are the amplitudes and angular frequencies, respectively. We observe that each frequency component in $v(t)$ is the same as in $x(t)$ but scaled by their angular frequency and phase delayed. Therefore, measuring $v(t)$ is equivalent to measuring $x(t)$, and since the Doppler shift is proportional to $v(t)$ according to Eq. (2), measuring the Doppler shift is analogous to measuring the vibrational signal:

$$x(t) = \sum_i A_i \sin(\omega_i t), \quad (5)$$

$$v(t) = \dot{x}(t) = \sum_i A_i \omega_i \cos(\omega_i t) = \sum_i A_i \omega_i \sin(\omega_i t + 90^\circ). \quad (6)$$

In our setup, we use a laser with a central wavelength of 1550 nm, capable of modulating its output frequency with a bandwidth, $B = 12.5$ GHz, and a period, $T = 2.5$ ms, corresponding to a modulation frequency of 400 Hz. Therefore, according to the Nyquist sampling theorem, we can measure Doppler signals, and thereby vibrational signals, modulating up to 200 Hz without aliasing effects. The detector used is an SNSPD with 80% detection efficiency for 1550 nm, 10 ns dead time, 19 ps timing jitter, <100 dark counts/second, and a maximum count rate of $\sim 10^6$ photons/second.

To determine the beating frequencies, we Fourier transform the detected photon count rate using the Welch method. It is similar to the standard *fast Fourier transform* (FFT) algorithm, but instead of transforming the entire data set as one, the Welch method uses a sliding window to split the signal into a series of overlapping segments. It performs an FFT of each segment and averages the resulting *power spectral density* (PSD) [21]. Using the Welch method, the noise in the Fourier space is decreased compared to FFT, but since each segment contains fewer samples, the spectral resolution is decreased [22].

Analysis and results. *Constant signals.* To demonstrate the system's ability to monitor vibrations, a continuous signal containing three frequencies (95, 135, and 175 Hz) is applied to the

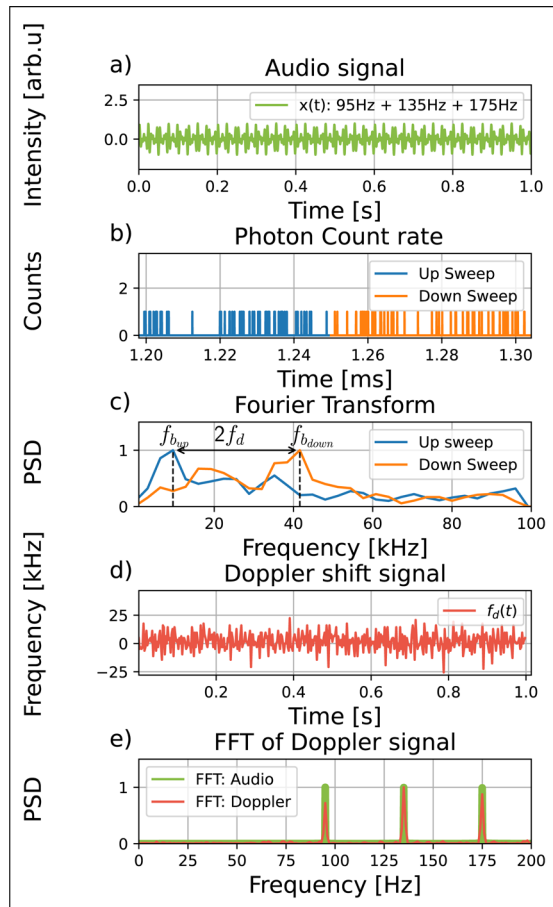


Fig. 2. (a) Constant multi-frequency audio signal applied to the speaker. (b) Single-photon count rate data (zoomed in) of the SNSPD from one frequency sweep. Marker signals from the laser allow for the splitting of up sweep and down sweep. (c) Fourier transform of the two count rate segments, displaying the beating frequencies of the up and down sweeps. (d) Doppler shift versus time; each data point is extracted as the difference between two consecutive up and down sweep beating frequencies. (e) Fourier transform of the time-dependent Doppler signal, demonstrating the successful reconstruction of the original speaker audio signal.

speaker as shown in Fig. 2(a). The laser emits a $\sim 1 \mu\text{W}$ probe signal and the resulting $\sim 10^6$ photons/second flux is measured and recorded over 1 s. Utilizing the marker signals from the laser, the count rate is split according to the up and down sweeps of the sawtooth laser modulation. With 400 Hz laser modulation, each up and down sweep is 1.25 ms in duration, and Fig. 2(b) displays a zoomed in and color-coded segment of the count rate data acquired over a single laser modulation period in a 10 ns bin size histogram. The bin size is set to match the dead time of the SNSPD to ensure that at most a single photon is present in each bin.

The count rates of the up and down sweeps are then Fourier transformed individually; using the Welch method [23] with a quarter-length window size and 50% overlap between segments, these settings were determined empirically to give the best result. Normalized, this produces the frequency spectra displayed in Fig. 2(c), for the up and down sweeps. Frequency components < 4 kHz are filtered out as they are the result of the non-coherent photon detections. The frequencies $f_{b_{up}}$ and

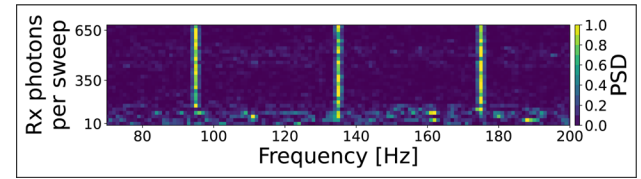


Fig. 3. Heatmap displaying multiple vibrational spectra measured using progressively fewer reflected photons per laser modulation sweep.

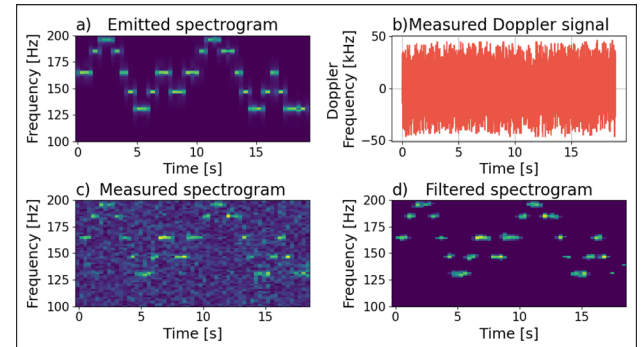


Fig. 4. (a) STFT spectrogram of the audio signal emitted by the speaker (a segment of Bach's 9th symphony: Ode to Joy). (b) Time-dependent Doppler signal measured with the setup. (c) STFT spectrogram of the measured Doppler signal. (d) Filtered STFT spectrogram using Gaussian smoothing and edge detection convolution filters.

$f_{b_{down}}$ are extracted from the spectra in Fig. 2(c) by taking the corresponding peak values. The distance, d , is acquired by taking the average $f_b = (f_{b_{down}} + f_{b_{up}})/2$ according to Eqs. (3) and (4) and using Eq. (1). Similarly, the momentary Doppler shift is extracted as $f_d = (f_{b_{down}} - f_{b_{up}})/2$ according to Eqs. (3) and (4). The process in Figs. 2(b) and 2(c) is repeated for all count rate data, producing Fig. 2(d), and displaying the measured Doppler shift over time, which, according to Eq. (6), is analogous to the audio signal applied to the speaker. To confirm that the Doppler shift is modulating synchronously with the applied signal shown in Fig. 2(a), the acquired Doppler signal is Fourier transformed and compared with the Fourier transform of the applied signal in Fig. 2(a). The resulting frequency spectra shown in Fig. 2(e) demonstrate that we successfully captured the signal in Fig. 2(a).

Lastly, we investigate the number of detected Rx photons required to determine a target's vibrational spectra using our setup. The measurement and analysis demonstrated in Fig. 2 are repeated while using progressively weaker laser signals, thereby acquiring weaker Tx and Rx signals. The results of the laser power sweep are displayed in Fig. 3, where each row corresponds to a vibrational spectra equivalent to Fig. 2(e) and the y axis represents the number of detected reflected photons. These results demonstrate the possibility to measure Doppler shifted signals using as few as 100 photons per laser sweep.

Time-dependent signals. To demonstrate the system's ability to monitor signals with time-dependent frequency components, the speaker emits a musical signal. The emitted signal's *short-time Fourier transform* (STFT) spectrogram, shown in Fig. 4(a), displays the audio frequencies over time. The FMCW setup again records the single-photon count rate, which is analyzed using the

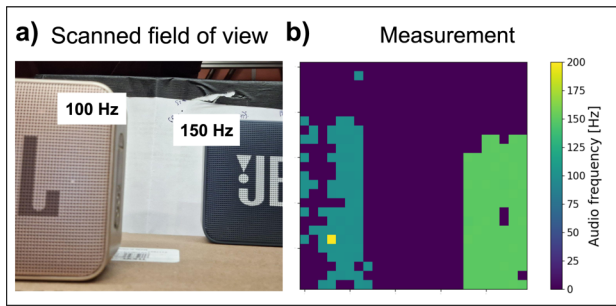


Fig. 5. (a) Scanned field of view including two speakers emitting audio signals of 100 and 150 Hz, respectively. (b) Heatmap displaying the measured audio frequencies from a scanned measurement.

method demonstrated in Figs. 2(b)–2(d), generating the measured Doppler signal in Fig. 4(b). The STFT spectrogram of the measured signal is displayed in Fig. 4(c), and when compared with the emitted spectrogram, the musical signal is visible, however with additional frequency noise. To reduce the noise in the measured signal, we generate a filter mask that comprises two simple convolution filters and apply it to the measured spectrogram: first, a Gaussian convolution filter with kernel size three for local smoothing and removing small gaps in the measured spectrogram [24], and second, a Sobel edge detection convolution filter to identify frequency components exhibiting stronger intensities compared with the background [25]. The resulting filtered spectrogram is displayed in Fig. 4(d) and the de-noised signal is recovered via inverse STFT.

Scanned images. Lastly, we demonstrate the system's ability to scan the probe signal across a scene to map vibrational frequencies in different regions. The scanned field of view is displayed in Fig. 5(a) with two speakers, each emitting a distinct audio signal (100 and 150 Hz, respectively), placed in front of a stationary background. The scan is performed with 0.5 s of integration time per point in a 25×25 grid. For each point scanned, the analysis described in Fig. 2 is performed, and the dominant frequency in Fig. 2(e) is extracted. The resulting heatmap of the measured audio frequencies is displayed in Fig. 5(b), where three distinct regions are visible, corresponding to the two speakers and the stationary background.

Conclusion and outlook. We have presented an FMCW LIDAR setup and demonstrated its ability to remotely measure vibrational spectra in 3D. By recording the single-photon flux and determining the time-dependent Doppler shift induced by the speaker's vibration, we measure audio signals with multiple fixed and time-dependent frequencies up to 200 Hz, limited by the laser's modulation periodicity of 2.5 ms, which determines the maximum audio frequency that can be acquired according to the Nyquist theorem. Utilizing an SNSPD allows for measurements to be performed at the single-photon level with high timing accuracy and efficiency. We demonstrate experimentally the possibility of measuring the momentary Doppler shifts with ≈ 100 detected reflected photons. This work paves

the way for advanced LIDAR applications in challenging and photon-starved conditions, opening the possibility of monitoring Doppler shifted signals from weakly scattering targets such as air (to determine wind speed), or measuring through lossy media such as water or a human tissue.

Funding. HORIZON EUROPE European Research Council (899824, (FET-OPEN, SURQUID)).

Acknowledgment. We wish to thank the Bachelor students Paula Schembri and Truls Svensson for contributing to this project.

Disclosures. The author Val Zwiller is a co-founder of the company Single Quantum that provided the detection system used in this project. The other authors declare no conflicts of interest.

Data availability. Data underlying the results presented in this article are available upon request.

REFERENCES

- V. Molebny, G. Kamerman, and O. Steinvall, *Electro-Optical Rem. Sens., Photon. Technol., Appl. IV* **7835**, 783502 (2010).
- C. M. Natarajan, M. G. Tanner, and R. H. Hadfield, *Supercond. Sci. Technol.* **25**, 063001 (2012).
- R. O. Dubayah and J. B. Drake, *J. For.* **98**, 44 (2000).
- Z. Ren, L. Wang, and L. Bi, *Sensors* **19**, 2915 (2019).
- M. Wilkinson, U. Schreiber, I. Procházka, *et al.*, *J. Geod.* **93**, 2227 (2019).
- J. Larsson, J. Bood, C. T. Xu, *et al.*, *Opt. Express* **27**, 17348 (2019).
- A. McCarthy, X. Ren, A. D. Frera, *et al.*, *Opt. Express* **21**, 22098 (2013).
- S. Yu, Z. Zhang, H. Xia, *et al.*, *Light: Sci. Appl.* **10**, 212 (2021).
- B. Behroozpour, P. A. Sandborn, M. C. Wu, *et al.*, *IEEE Commun. Mag.* **55**, 135 (2017).
- A. Kirmani, D. Venkatraman, D. Shin, *et al.*, *Science* **343**, 58 (2014).
- N. Hu, Y. Meng, K. Zou, *et al.*, *Optica* **9**, 346 (2022).
- H. Wu, Y. Li, W. Xu, *et al.*, *Nat. Commun.* **15**, 345 (2024).
- F. Zhang, L. Yi, and X. Qu, *Opt. Commun.* **474**, 126066 (2020).
- S. Suyama, H. Ito, R. Kurahashi, *et al.*, *Opt. Express* **29**, 30727 (2021).
- D. V. Reddy, R. R. Nerem, S. W. Nam, *et al.*, *Optica* **7**, 1649 (2020).
- R. H. Hadfield, J. Leach, F. Fleming, *et al.*, *Optica* **10**, 1124 (2023).
- A. M. Pawlikowska, A. Halimi, R. A. Lamb, *et al.*, *Opt. Express* **25**, 11919 (2017).
- B. Korzh, Q. Y. Zhao, J. P. Allmaras, *et al.*, *Nat. Photonics* **14**, 250 (2020).
- K. Zou, Z. Hao, Y. Feng, *et al.*, *Opt. Lett.* **48**, 415 (2023).
- M. G. Tanner, T. R. Choudhary, T. H. Craven, *et al.*, *Biomed. Opt. Express* **8**, 4077 (2017).
- E. L. Nylen and P. Wallisch, *Neural Data Science: A Primer with MATLAB and Python* (Academic Press, 2017).
- P. Welch, *IEEE Trans. Audio Electroacoust.* **15**, 70 (1967).
- "SciPy Welch," <https://docs.scipy.org/doc/scipy/reference/generated/scipy.signal.welch.html>. [Accessed 21-08-2024].
- "SciPy Gaussian filter," https://docs.scipy.org/doc/scipy/reference/generated/scipy.ndimage.gaussian_filter.html. [Accessed 21-08-2024].
- A. C. Bovik, *The Essential Guide to Image Processing* (Academic Press, 2009), Chap. 19, pp. 506–507.